JACS
JOURNAL OF THE AMERICAN CHEMICAL SOCIETY
Article
pubs.acs.org/JACS

Selective Chemical Imaging of Static Actin in Live Cells

Lech-Gustav Milroy,[#,⊥,†,‡] Stefano Rizzo,[#,⊥,‡] Abram Calderon,[▽,⊥] Bernhard Ellinger,[#,⊥] Silke Erdmann,[#] Justine Mondry,[▽] Peter Verveer,[▽] Philippe Bastiaens,[▽,⊥] Herbert Waldmann,[*,#,⊥] Leif Dehmelt,[*,▽,⊥] and Hans-Dieter Arndt*[,#,∥]

[#]Department of Chemical Biology and [▽]Department of Systemic Cell Biology, Max-Planck-Institute of Molecular Physiology, Otto-Hahn-Straße 11, 44227 Dortmund, Germany

[⊥]Faculty of Chemistry, Technische Universität Dortmund, Otto-Hahn-Straße 6, 44221 Dortmund, Germany

[∥]Institute of Organic and Macromolecular Chemistry, Friedrich-Schiller-Universität Jena, Humboldtstraße 10, 07743 Jena, Germany

Supporting Information

ABSTRACT: We have characterized rationally designed and optimized analogues of the actin-stabilizing natural products jasplakinolide and chondramide C. Efficient actin staining was achieved in fixed permeabilized and non-permeabilized cells using different combinations of dye and linker length, thus highlighting the degree of molecular flexibility of the natural product scaffold. Investigations into synthetically accessible, non-toxic analogues have led to the characterization of a powerful cell-permeable probe to selectively image static, long-lived actin filaments against dynamic F-actin and monomeric G-actin populations in live cells, with negligible disruption of rapid actin dynamics.

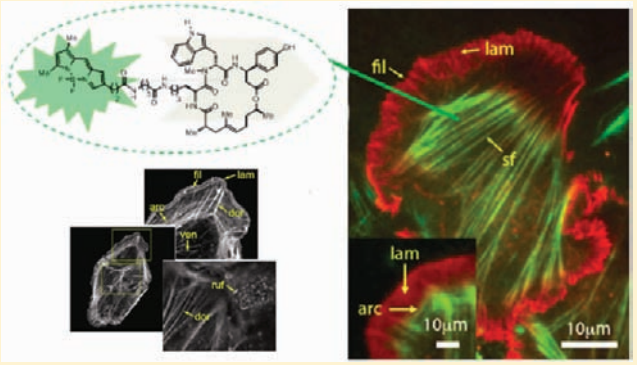

INTRODUCTION

The tightly regulated, dynamic equilibrium between monomeric (G-actin) and helical-filamentous (F-actin) structures is a key component of important cellular functions in normal and pathological states[1,2] that impacts cell motility, endocytosis, and cytokinesis. Means to image actin, primarily by fluorescence-based microscopy, have become indispensable for studying actin and its interaction with cell components.[3−5] Furthermore, attachment of fluorescent reporters to small-molecule probes has been applied very successfully for target elucidation studies by using comparative cell microscopy[6−8] or high-content screening.[9−12]

In fixed, permeabilized cells, typical actin structures can be imaged *post mortem* by using fluorescent labels either on anti-actin antibodies[12−14] or on phalloidins (**1**, Figure 1),[15] small molecule heptapeptide toxins from the death cap mushroom *Amanita sp*. Labeled phalloidins have helped to shape our current knowledge about actin cell biology.[16,17] Today, semi-synthetic fluorescent conjugates of phalloidin (Figure 1, e.g., **2** and **3**) are widely used, as they selectively bind to the F-actin quaternary structure and do not label the G-actin pool. Most actin antibodies fail to discriminate between those pools and hence suffer from a comparatively high background signal due to abundant, cytosolic G-actin.

In live cells, actin structures can be observed either by microinjecting fluorescently labeled actin proteins into living cells or by overexpressing a fusion protein composed of G-actin and a fluorescent protein, such as green fluorescent protein (GFP).[18,19] Human cell lines are routinely transfected with DNA vectors for such fusion proteins. However, for primary cells, tissues, and many non-mammalian cells, transfection is often difficult, impractical, or unreliable. Moreover, overexpression of GFP-tagged actin is known to interfere with cytoskeletal dynamics, causing aberrations in myosin processivity and slight impairment in cytokinesis.[19] Fluorescently tagged F-actin binding proteins or peptides were introduced as a less disturbing method[20,21] but still are not independent of DNA transfer technology. Thus, more versatile probes could be extremely useful for unrestricted monitoring of actin structures in native cells.

Similar to phalloidin (**1**), the cyclodepsipeptide natural products jasplakinolide (or "jaspamide", **4**) and chondramide C (**5**, Figure 1) were found to stabilize F-actin, resulting in potent (nanomolar) cytotoxicity.[22−26] Convincing evidence suggests that **1**, **4**, and **5** target a similar binding site on F-actin.[27] Interestingly, **4** and **5** were considered for therapeutic applications[28−30] but have not yet been developed further.[31] However, even with a low therapeutic index, these compounds could prove to be excellent probes for scientific applications. In contrast to phalloidin,[32] **4** and **5** freely penetrate cells and can be effectively prepared by total synthesis.[33−43] Moreover, by targeted structural variation, high acute toxicity might be reduced to improve applicability in live cell studies. Most importantly, such probes should have a high propensity to enter

Received: January 3, 2012
Published: April 4, 2012

dx.doi.org/10.1021/ja211708z | J. Am. Chem. Soc. 2012, 134, 8480−8486

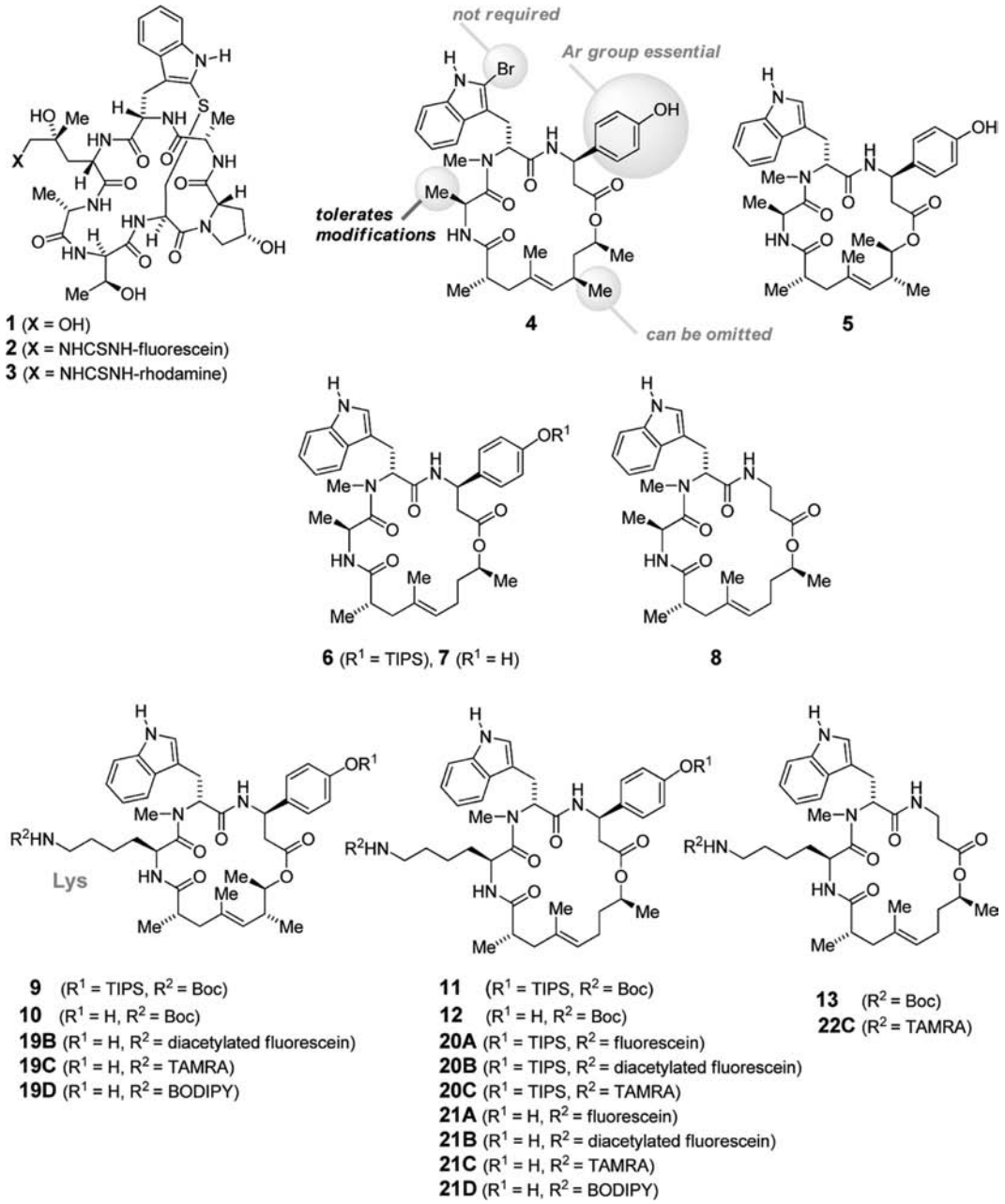

Figure 1. Chemical structures of phalloidin (**1**), typical phalloidin conjugates (**2**, **3**), jasplakinolide (**4**), chondramide C (**5**), simplified cyclodepsipeptide analogues **6**–**8**, and Boc-protected lysine analogues **9**–**13** for conjugation studies as well as fluorescently labeled conjugates **19**–**22**. The phalloidin skeleton is depicted in a projection similar to **4** and **5**, suggesting common functional regions. **4** and **5** may hence be regarded as natural *retro-inverso* peptide mimetics of **1**, at least concerning the crucial indole pharmacophore. Key variation areas are indicated on **4**.

living cells, potentially providing generic actin-targeting tools for cell microscopy.

■ COMPOUND DESIGN

To serve as a probe platform, the natural product lead structures **4** and **5** had to be simplified as much as possible. Previous studies indicated that the 2-Br substituent on the indole ring was not required and that one aliphatic Me-group of the polyketide section might be omitted to afford similarly efficacious actin modulators.[42] Subsequent scrutiny of structure–activity trends for derivatives of **4** and **5** suggested that modification of the Ala methyl residue should be tolerated (Figure 1).[42,44–46] According to our binding model for **4** and **5**,[42,43] this residue would correspond to the dihydroxy-Leu side chain of phalloidin (**1**). On **1**, this residue served as a benign point of attachment for reporter groups. Furthermore, compelling data on the binding of TRITC-[47] and undecagold-labeled phalloidin[48] suggest that these reporter groups are located outside the binding cleft.

■ RESULTS

Following this rationale, lysine analogues **10** and **12** (Figure 1) were prepared[42,43] by replacing the Ala residue with an ε-Boc-protected Lys. Triisopropylsilyl (TIPS)-protected analogues **9** and **11** as well as a β-Ala-derived **13** were synthesized as controls (Figure 1). Based on earlier data,[42] these compounds were expected to display much lower binding affinity toward actin than **10** and **12**. Indeed, cell viability studies (Table 1) showed that the *O*-TIPS (**9** and **11**) and β-Ala (**13**) analogues were inactive up to the highest applied concentration (15/30 μM) or orders of magnitude less active—mirroring the

dx.doi.org/10.1021/ja211708z | J. Am. Chem. Soc. 2012, 134, 8480–8486

Table 1. Cytotoxicity Data

	IC_{50}/nM	
compd	MCF-7	HT-29
4	25 ± 4	21 ± 4
5	23 ± 2	21 ± 1
6	$1.8 \times 10^4 \pm 1.1 \times 10^4$	$1.8 \times 10^4 \pm 0.8 \times 10^4$
7	40 ± 3	26 ± 1
8	$>1.5 \times 10^4$	$>1.5 \times 10^4$
9	$>1.5 \times 10^4$	$>1.5 \times 10^4$
10	37 ± 4	28 ± 3
11	$>3 \times 10^4$	$>3 \times 10^4$
12[a]	39 ± 39	10 ± 4
13	$2.0 \times 10^3 \pm 0.1 \times 10^3$	$8.2 \times 10^3 \pm 1.9 \times 10^3$

[a]This compound showed an unconventional toxicity pattern; only the first IC_{50} is listed

structure–activity trends observed for their Ala counterparts **6** and **8**. Compounds **10** and **12**, however, were equally cytotoxic toward MCF7 and HT-29 cell lines as the parental natural compounds **4** and **5** (Table 1).

Synthesis of Fluorescent Conjugates. These data strengthened the pharmacophore hypothesis and proved that scaffold modification was benign. Next, we sought to test whether appending additional functional groups to the lysine side chain could be tolerated. To enable the identification of live-cell actin probes, a small collection of dye conjugates was prepared (Figure 2 and Scheme S1). These compounds were synthesized by acid-mediated Boc-group deprotection of **10** or **12**, followed by NHS-activated amide coupling (Figure 2), and purified by preparative HPLC in yields of 13–92% over the two steps. Fluorescently labeled analogues of **9**, **11**, and **13** were also prepared for control studies (Figure 2).

Fluorescent Labeling of F-Actin in Fixed Cells. Initial analysis of staining efficiency revealed that fluorescently labeled compounds **19** and **21**—based on the active compounds **10** and **12**, respectively—could selectively and efficiently stain F-actin in several mammalian cell lines after fixation (Figure 2c and Figure S1). In fact, in N2a, BSC-1, and HeLa cells, characteristic and intense labeling of actin-rich filopodia, lamellipodia, and actin bundles was observed after incubation with **19B**, **19C**, **19D**, **21B**, and **21C** (see Figure S1). In contrast, TAMRA-labeled probes **20B**, **20C**, and **22C**—derived from the inactive compounds **11** and **13**—did not selectively stain F-actin (see Figure S1). Next, more extensive confocal microscopy studies of stained human osteosarcoma U2OS cells were performed on a subset of probes (Figure 3). TAMRA-labeled analogues **19C** and **21C** visualized typical actin structures in maximum projections of Z-stacks. While cell staining at 1 μM **19C** was weak without permeabilization, the staining efficiency of **21C** at the same concentration was independent of permeabilization. Neither **20C** nor **22C** (both at 10 μM) was capable of selectively labeling F-actin; only membranous structures were stained (Figure 3a). The overall labeling patterns were very similar in the cases where fixed and permeabilized U2OS cells were simultaneously co-stained with labeled phalloidin and labeled probes **21C**, **21D**, and **19C** (Figure 3b). Direct comparison of individual Z-sections near (bottom) and far (top) from the glass substrate in the two regions of interest revealed that Alexa-488 phalloidin and **19C** both labeled the same actin structures, including filopodia, lamellipodia, transversal arcs, dorsal stress fibers, ventral stress fibers, and dorsal ruffles (Figure 3c). No staining preference among these structures was observed for either of the two probes.

Selective Labeling of Long-Lived F-Actin Structures in Living Cells. Our observation that non-permeabilized, fixed U2OS cells were efficiently stained by the TAMRA-labeled analogue **21C** prompted us to investigate living cells. After transfection and expression of a dominant-positive mutant of the small GTPase Rac1, Neuro-2a neuroblastoma (N2a) cells[49] form extensive, dynamic lamellipodia and filopodia, as well as less dynamic, long-lived stress fibers and dynamically intermediate actin arc structures (Figure 4a). Therefore, these cells seemed optimally suited to evaluate the interaction of our novel fluorescent probes with F-actin structures characterized by distinct dynamic turnover rates. Although the TAMRA-labeled analogue **21C** was able to efficiently stain non-permeabilized, fixed U2OS cells, no significant staining of living N2a cells by the same probe could be detected following

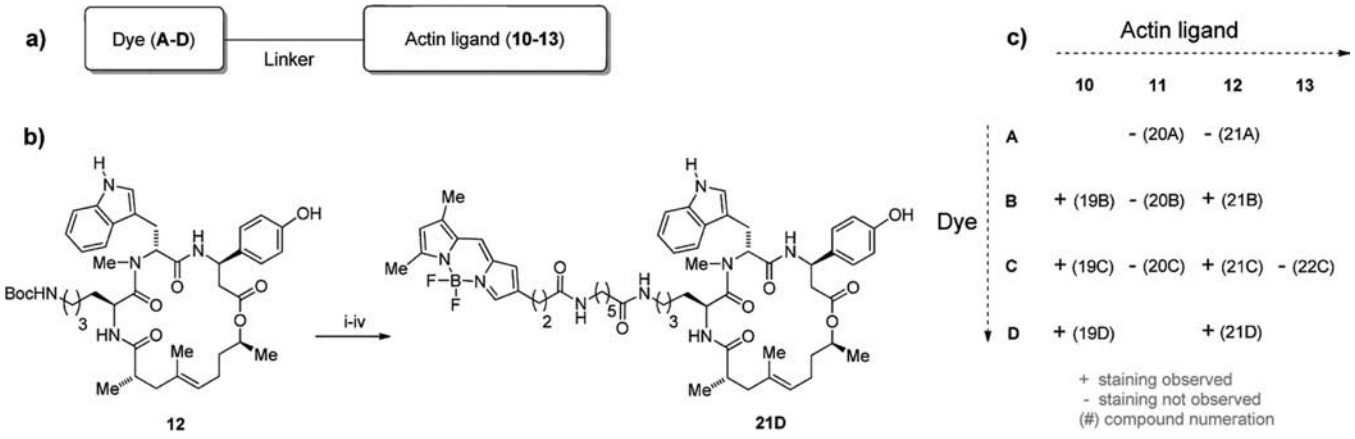

Figure 2. (a) Generic probe setup. (b) Synthesis of dye conjugates. Reagents and conditions: (i) 30% CF_3COOH/CH_2Cl_2 (v/v), 1 h, rt; (ii) 6-(*tert*-butoxycarbonylamino)hexanoic acid, HOAt, HATU, *N*-methylmorpholine, DMSO, rt, overnight; (iii) 30% CF_3COOH/CH_2Cl_2 (v/v), 1 h, rt; (iv) BODIPY-FL, HOAt, HATU, *N*-methylmorpholine, DMSO, 14 h, rt, 26% over four steps (for **21D**). (c) Actin probe library (**19**–**22**) and a staining efficacy map (see Figures S1 and S2). Dye conjugates: **A** = fluoresceine 5-carboxylate; **B** = diacetyl fluoresceine 5-carboxylate; **C** = TAMRA (tetramethylrhodamine 5/6-carboxylate); **D** = BODIPY-FL (*β*-4,4-difluoro-5,7-dimethyl-4-bora-3*a*,4*a*-diaza-*s*-indacenyl propionate). Compound **20A** was only tested in preliminary experiments.

dx.doi.org/10.1021/ja211708z | *J. Am. Chem. Soc.* 2012, 134, 8480–8486

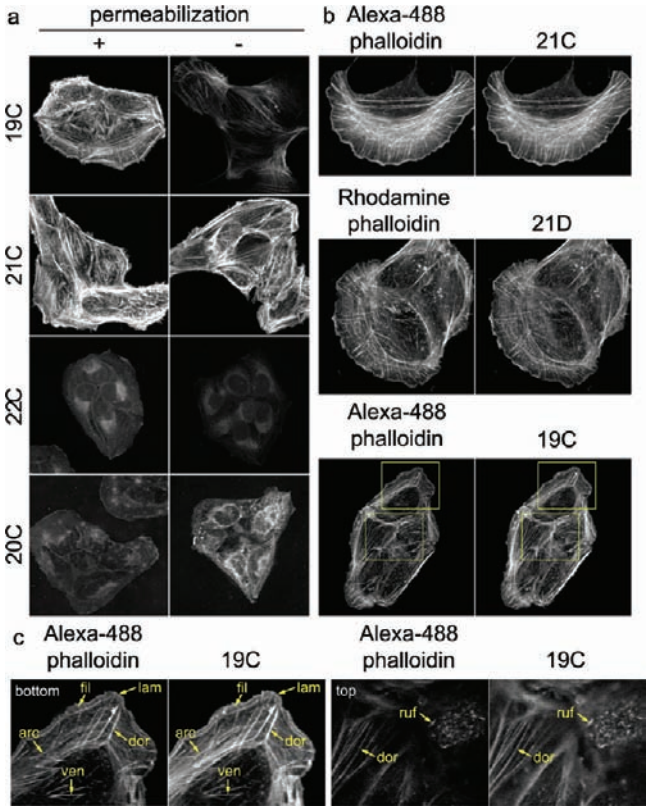

Figure 3. Representative images of fixed U2OS cells stained with labeled jasplakinolide analogues. (a) U2OS cells were fixed and stained either with (+) or without (−) cell permeabilization and imaged using confocal microscopy. (b) Fixed and permeabilized U2OS cells were co-stained with spectrally distinguishable labeled phalloidin and labeled jasplakinolide analogues. Maximum projections of Z-stacks are shown. (c) Individual Z-sections near (bottom) and far (top) from the glass substrate from two regions of interest highlighted in (b). Due to their different spectral properties, the resolution in the *z*-plane was lower for the red-shifted TAMRA dye than for Alexa-488. Therefore, more structures were visible outside the plane of focus when using the TAMRA probe **19C**. Abbreviations: fil, filopodia; lam, lamellipodia; arc, transversal arcs; dor, dorsal stress fibers; ven, ventral stress fibers; and ruf, dorsal ruffles.

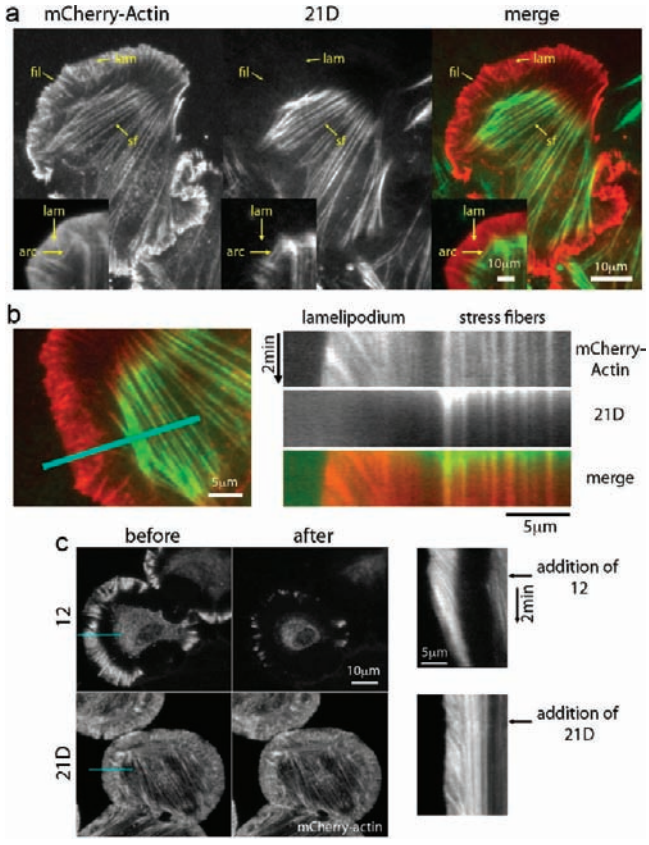

Figure 4. Representative images of living Neuro-2a cells treated with jasplakinolide probes **12** and **21D**. (a) Living Neuro-2a cells coexpressing a nonlabeled dominant positive mutant (Q61L) of Rac1 and actin fused to mCherry were incubated with **21D** (10 μM) for 5 min in imaging medium, extensively washed, and subjected to TIRF microscopy. Five minute incubation with 1 μM **21D** was sufficient for weaker staining intensity. (b) Kymograph analysis of dynamic and static actin structures. Left: Line indicating the cell region used for kymograph analysis. Right: Kymograph of mCherry-actin shows dynamic retrograde actin flow in lamellipodia (diagonal lines) and stable actin structures in stress fibers (vertical lines). Only the stable actin structures are labeled with **21D** (see also Supplementary Movie S1). (c) Effect of **12** (unlabeled) and **21D** (BODIPY labeled) on actin dynamics. Left: Images (mCherry actin channel) before and 5 min after compound application. Right: Kymograph analysis of actin dynamics during compound application (see also Supplementary Movie S2). Abbreviations: fil, filopodia; lam, lamellipodia; arc, transversal arcs; sf, stress fibers.

a brief exposure and washout (see Figure S2). By contrast, the BODIPY-labeled analogues **19D** and **21D** were capable of efficient and selective labeling of F-actin in living cells (see Figure S1 and Figure 4a, respectively). We briefly examined the spectrocopical properties of probe **21D** (fluorescence absorption, emission, quantum yield), which we found mildly modified when compared to the isolated BODIPY-FL chromophore and similar to BODIPY-labeled natural product molecules. (See Supporting Information for details.)

These observations encouraged us to further investigate the full capability of these probes in more extensive live cell studies using only the synthetically most accessible variant, i.e. **21D**. Analysis using total internal reflection fluorescence (TIRF) microscopy[50] clearly showed that long- or intermediate-lived structures, such as stress fibers or actin arcs (Figure 4a), were strongly labeled by **21D**. In contrast, highly dynamic structures undergoing rapid turnover, such as lamellipodia or filopodia, were not labeled by **21D**, although they were clearly indicated by overexpressed mCherry-actin (Figure 4a). Under the imaging conditions applied (30 ms exposure with a 488 nm laser in TIRF mode, image acquisition every 3 s), the BODIPY label in **21D** bleached to 50% of its original intensity after 8.3 acquisitions.

Probe dissociation did not occur at this time scale, as non-illuminated neighboring cells were largely unaffected. In fact, labeled cells could be observed for at least 3 h after probe washout. This suggests that **21D** has a slow turnover on actin filaments in cells. To assess probe turnover more directly, we used fluorescence recovery after photobleaching (FRAP). As **21D** selectively labels actin structures with a relatively slow filament turnover, such as transversal arcs and ventral stress fibers, we focused on bleaching cell areas that predominantly contained those structures (Figure S3). However, in any region of the cell, actin ruffles or focal contacts characterized by fast filament turnover were also present at a minor fraction. The apparent recovery rate of mCherry-actin was relatively slow, with k_m(mCherry-Actin) = 0.17 ± 0.03 min^{-1}, and similar to

dx.doi.org/10.1021/ja211708z | *J. Am. Chem. Soc.* 2012, 134, 8480−8486

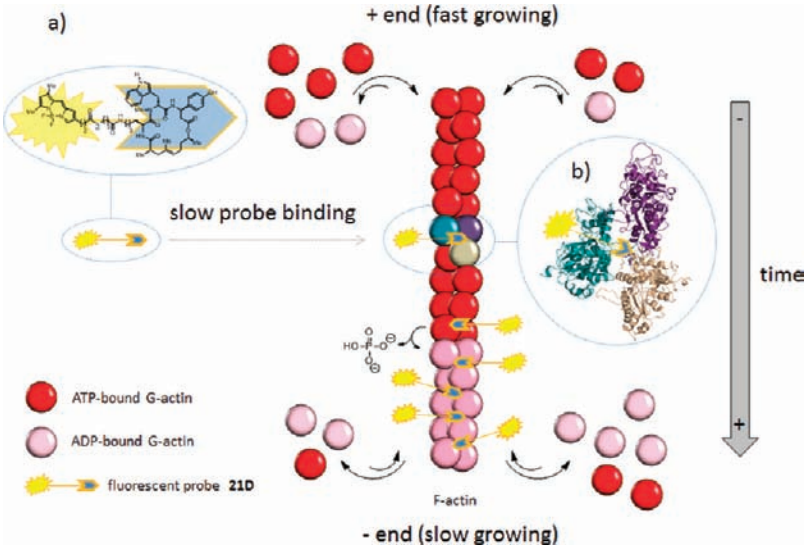

Figure 5. (a) Simplified schematic overview of the actin polymerization process and the preferred staining of long-lived actin structures. F-actin is stabilized by ATP hydrolysis. (b) Proposed binding model.[43] The cyclodepsipeptide ligand **21D** binds to and stabilizes the actin filaments at a point of contact between three G-actin monomers, with the BODIPY dye presumably protruding into the solvent. Due to the slow on-rate of **21D** binding to F-actin, short-lived, more dynamic actin structures are labeled much more weakly compared to long-lived, less dynamic actin structures.

previously reported recovery rates of actin in ventral stress fibers of U2OS cells.[51] Recovery of **21D** was slightly slower (k_{21D} = 0.14 ± 0.04 min^{-1}) but similar to the actin recovery rate.

Actin filaments in transversal arcs and ventral stress fibers are thought to mainly originate from preformed filaments and not from *de novo* polymerization.[51] Thus, the simultaneous recovery of both the mCherry-actin and **21D** signals is compatible with the notion that mCherry-actin filaments already labeled with **21D** recover concurrently in transversal arcs and ventral stress fibers. It is unclear if **21D** also has a significant turnover between actin filaments and the cytosol, but our FRAP measurements reveal an upper limit for the apparent recovery rate constant and suggest that the observed turnover rate of **21D** in cells must be slower than or equal to 0.14 ± 0.04 min^{-1} (i.e., $t_{1/2} \geq$ 4.95 min).

Importantly, video microscopy and kymograph analysis of living cells labeled with probe **21D** showed that F-actin remained highly dynamic in lamellipodia (Figure 4b and Supplementary Movie S1), despite the presence of the jasplakinolide-derived probe. This stands in stark contrast to the natural product **4**, which is widely documented to induce a rapid collapse of dynamic F-actin structures.[52,53] In control experiments, unlabeled compound **12** (10 μM) also inhibited actin dynamics shortly after application and induced immediate collapse of lamellipodia, while **21D** did not (Figure 4c and Supplementary Movie S2), suggesting that the fluorescent label in **21D** reduces the compound's actin disturbing activity. Indeed, **21D** did not provoke any noticeable change in actin dynamics or cell morphology at the applied concentration of 10 μM. Furthermore, cytotoxicity measurements in Neuro-2a cells showed that both labeled compounds **21C** and **21D** had no impact on cell growth or on cell survival when applied at concentrations up to 60 μM for 3 days.

■ DISCUSSION

Our results strongly indicate that synthetic cyclodepsipeptides inspired by natural actin binders such as jasplakinolide (**4**) or chondramide C (**5**) can provide powerful tools for investigating F-actin. In fact, when opportunely modified using solid-phase-based total synthesis[45] and outfitted with an appropriate dye, characteristic and intense labeling of actin-rich structures can be achieved in a highly practical fashion in live cells. Moreover, the staining pattern observed with our synthetic fluorescent probes strengthens our previous pharmacophore model for cyclodepsipeptide-based actin ligands.[42] Notably, an appropriate balance between actin–ligand affinity and dye characteristics seems mandatory. Selective labeling of actin structures in live cells was only possible with the BODIPY-modified analogues **19D** and **21D**. Among several dye moieties tested, BODIPY emerged as a suitable candidate, likely stemming from its small molecular weight, neutral charge, and appropriate lipophilicity. BODIPY has been used in a number of commercially available natural-product-based staining reagents (Figure S4). However, we specifically note that the compounds described here are fully synthetic and different from jaspamide or chondramide C, and have been a result of scrutinizing SAR data and multifactorial optimization. While further investigations are certainly needed to clarify why **21D** is apparently non-toxic and does not affect actin dynamics on the time scale of typical microscopic analysis (hours), it retained the excellent cell permeability and actin-binding properties of the parental natural product. Therefore, long-lived filamentous actin can be visualized with high sensitivity upon standard and readily performed incubation and washing procedures, without recourse to genetic or single-cell manipulations.

During actin polymerization, globular monomeric actin (G-actin) loaded with ATP preferentially adds to the fast growing plus-ends of existing actin filaments (F-actin, Figure 5a). The dye-labeled probe (e.g., **21D**) is expected to bind F-actin with a relatively slow on-rate[54] due to the rather concealed binding region at the junction of three actin protein monomers (see Figure 5b). Similar to an earlier study using labeled phalloidins to stain actin in neuronal growth cones,[55] our novel probes also stain highly dynamic, short-lived filament populations (such as in lamellipodia or filopodia), considerably weaker than long-lived filament populations (such as in stress fibers and actin arcs). However, unlike labeled phalloidins, which need to be

dx.doi.org/10.1021/ja211708z | J. Am. Chem. Soc. 2012, 134, 8480–8486

microinjected into living cells, our probes are freely cell permeable.

CONCLUSION AND PERSPECTIVES

We have characterized rationally designed and optimized analogues of the actin-stabilizing natural products jasplakinolide and chondramide C. The potential of these less-toxic analogues as cell-permeable actin probes has been explored through the attachment of different fluorophores. Efficient actin staining was achieved in fixed permeabilized and non-permeabilized cells using different combinations of dye and linker length, thus highlighting the degree of molecular flexibility of the natural product scaffold. Most significantly, two of the probes tested (BODIPY analogues **19D** and **21D**) were found to be sufficiently cell-permeable for use in live cell experiments. Subsequent investigations into the synthetically more accessible **21D** analogue led to the characterization of a powerful cell-permeable probe to selectively highlight static long-lived actin filaments, with negligible disruption of rapid actin dynamics.

Importantly, these probes can be generally prepared using an efficient and scalable total synthesis protocol, which potentially supersedes less accessible phalloidin derivatives based on material from a difficult-to-cultivate natural source. These data are expected to facilitate cell biology, imaging, or screening campaigns where genetic manipulation is otherwise not feasible or unavailable, and to generate insights into actin structure and dynamics in a generic fashion.

ASSOCIATED CONTENT

Supporting Information

Additional figures, video footage of cell treatment including legends, experimental procedures for cell manipulation and microscopy, chemical synthesis of new compounds, photophysical parameters of the probe **21D**, and ^{1}H and ^{13}C NMR spectra. This material is available free of charge via the Internet at http://pubs.acs.org.

AUTHOR INFORMATION

Corresponding Author

hd.arndt@uni-jena.de; leif.dehmelt@mpi-dortmund.mpg.de; herbert.waldmann@mpi-dortmund.mpg.de

Present Address

[†]Division of Molecular Bioengineering & Molecular Imaging, Eindhoven University of Technology, Eindhoven, The Netherlands

Author Contributions

[‡]L.-G.M. and S.R. contributed equally.

Notes

The authors declare no competing financial interest.

ACKNOWLEDGMENTS

This work was supported in part by the European commission (FP6, RTN ENDOCYTE). L.G.M. received a postdoctoral fellowship from the Alexander-von-Humboldt foundation. We thank M. Sc. L. Radke (TU Dortmund) for a donation of BODIPY carboxylic acid, G. Bokoch (TSRI, La Jolla, CA) for a plasmid coding for dominant positive Rac1 Q61L, M. Sc. V. Hannak (TU Dortmund) for a plasmid coding for mCherry-actin, M. Sc. M. Gräßl (U Duisburg-Essen) for providing fixed U2OS cells, M. Sc. A. Werkmüller (TU Dortmund) for support with quantum yield determination, and Profs. R. Winter and C. Czeslik (TU Dortmund) for access to fluorescence spectroscopy.

REFERENCES

(1) Disanza, A.; Steffen, A.; Hertzog, M.; Frittoli, E.; Rottner, K.; Scita, G. *Cell. Mol. Life Sci.* **2005**, *62*, 955.
(2) Schmidt, A.; Hall, M. N. *Annu. Rev. Cell Dev. Biol.* **1998**, *14*, 305.
(3) Small, J.; Rottner, K.; Hahne, P.; Anderson, K. I. *Microsc. Res. Tech.* **1999**, *47*, 3.
(4) Rodriguez, O. C.; Schaefer, A. W.; Mandato, C. A.; Forscher, P.; Bement, W. M.; Waterman-Storer, C. M. *Nat. Cell Biol.* **2003**, *5*, 599.
(5) Bugyi, B.; Carlier, M. F. *Annu. Rev. Biophys.* **2010**, *9*, 449.
(6) Alexander, M. D.; Burkart, M. D.; Leonard, M. S.; Portonovo, P.; Liang, B.; et al. *ChemBioChem* **2006**, *7*, 409.
(7) Schoof, S.; Pradel, G.; Aminake, M. N.; Ellinger, B.; Baumann, S.; Potowski, M.; Najajreh, Y.; Kirschner, M.; Arndt, H.-D. *Angew. Chem., Int. Ed.* **2010**, *49*, 3317.
(8) Quideau, S.; Douat-Casassus, C.; Delannoy Lopez, D. M.; Di Primo, C.; Chassaing, S.; Jacquet, R.; Saltel, F.; Genot, E. *Angew. Chem., Int. Ed.* **2011**, *50*, 5099.
(9) Abraham, V. C.; Taylor, D. L.; Haskins, J. R. *Trends Biotechnol.* **2004**, *22*, 15.
(10) Bleicher, K. H.; Böhm, H. J.; Müller, K.; Alanine, A. I. *Nat. Rev. Drug Discov.* **2003**, *2*, 369.
(11) Sumiya, E.; Shimogawa, H.; Sasaki, H.; Tsutsumi, M.; Yoshita, K.-i.; Ojika, M.; Suenaga, K.; Uesugi, M. *ACS Chem Biol.* **2011**, *6*, 425.
(12) Matus, A.; Ackerman, M.; Pehling, G.; Byers, H. R.; Fujiwara, K. *Proc. Natl. Acad. Sci. U.S.A.* **1982**, *79*, 7590.
(13) Kuczmarski, E. R.; Rosenbaum, J. L. *J. Cell. Biol.* **1979**, *80*, 356.
(14) Ab-El-Basset, E. M.; Fedoroff, S. *J. Chem. Neuroanat.* **1994**, *7*, 113.
(15) Wulf, F.; Deboben, A.; Bautz, F. A.; Faulstich, H.; Wieland, T. H. *Proc. Natl. Acad. Sci. U.S.A.* **1979**, *76*, 4498.
(16) Wieland, T. *Science* **1968**, *159*, 946.
(17) Lengsfeld, A. M.; Löw, I.; Wieland, T.; Dancker, P.; Hasselbach, W. *Proc. Natl. Acad. Sci. U.S.A.* **1974**, *71*, 2803.
(18) Choidas, A.; Jungbluth, A.; Sechi, A.; Murphy, J.; Ullrich, A.; Marriott, G. *Eur. J. Cell Biol.* **1998**, *77*, 81.
(19) Westphal, M.; Jungbluth, A.; Heidecker, M.; Mühlbauer, B.; Heizer, C.; Schwartz, J.-M.; Marriott, G.; Gerisch, G. *Curr. Biol.* **1997**, *7*, 176.
(20) Riedl, J.; Crevenna, A. H.; Kessenbrock, K.; Haochen, Y. J.; Neukirchen, D.; Bista, M.; Bradke, F.; Jenne, D.; Holak, T. A.; Werb, Z.; Sixt, M.; Wedlich-Soldner, R. *Nat. Methods* **2008**, *5*, 605.
(21) Pang, K. M.; Lee, E.; Knecht, D. *Curr. Biol.* **1998**, *8*, 405.
(22) Crews, P.; Manes, L. V.; Boehler, M. *Tetrahedron Lett.* **1986**, *27*, 2797.
(23) Crews, P.; Farias, J. J.; Emrich, R.; Keifer, P. A. *J. Org. Chem.* **1994**, *59*, 2932.
(24) Talpir, R.; Benayahu, Y.; Kashman, Y.; Pannell, L.; Schleyer, M. *Tetrahedron Lett.* **1994**, *35*, 4453.
(25) Zabriskie, T. M.; Klocke, J. A.; Ireland, C. M.; Marcus, A. H.; Molinski, T. F.; Faulkner, D. J.; Xu, C.; Clardy, J. *J. Am. Chem. Soc.* **1986**, *108*, 3123.
(26) Chevallier, C.; Richardson, A. D.; Edler, M. C.; Hamel, E.; Harper, M. K.; Ireland, C. M. *Org. Lett.* **2003**, *5*, 3737.
(27) Bubb, M. R.; Senderowicz, A. M. J.; Sausville, E. A.; Duncan, K. L. K.; Korn, E. D. *J. Biol. Chem.* **1994**, *269*, 14869.
(28) Senderowicz, A. M. J.; Kaur, G.; Sainz, E.; Laing, C.; Inman, W. D.; Rodriguez, J.; Crews, P.; Malspeis, L.; Grever, M. R.; Sausville, E. A.; Duncan, K. L. K. *J. Natl. Cancer Inst.* **1995**, *87*, 46.
(29) Stingl, J.; Andersen, R. J.; Emerman, J. T. *Cancer Chemother. Pharmacol.* **1992**, *30*, 401.
(30) Odaka, C.; Sanders, M. L.; Crews, P. *Clin. Diagn. Lab. Immunol.* **2000**, *7*, 947.
(31) Newman, D. J.; Cragg, G. M.; Holbeck, S.; Sausville, E. A. *Curr. Cancer Drug Targets* **2002**, *2*, 279.
(32) Schuresko, L. A.; Lokey, R. S. *Angew. Chem., Int. Ed.* **2007**, *46*, 3547.

(33) Grieco, P. A.; Hon, Y. S.; Perez-Medrano, A. *J. Am. Chem. Soc.* **1988**, *110*, 1630.
(34) Schmidt, U.; Siegel, W.; Mundinger, K. *Tetrahedron Lett.* **1988**, *29*, 1269.
(35) Chu, K. S.; Negrete, G. R.; Konopelski, J. P. *J. Org. Chem.* **1991**, *56*, 5196.
(36) Hirai, Y.; Yokota, K.; Momose, T. *Heterocycles* **1994**, *39*, 603.
(37) Imaeda, T.; Hamada, Y.; Shioiri, T. *Tetrahedron Lett.* **1994**, *35*, 591.
(38) Ghosh, A. K.; Moon, D. K. *Org. Lett.* **2007**, *9*, 2425.
(39) Tannert, R.; Hu, T.-S.; Arndt, H.-D.; Waldmann, H. *Chem. Commun.* **2009**, *12*, 1493.
(40) Hu, T.-S.; Tannert, R.; Arndt, H.-D.; Waldmann, H. *Chem. Commun.* **2007**, *38*, 3942.
(41) Zhdanko, A.; Schmauder, A.; Ma, C. I.; Sibley, L. D.; Sept, D.; Sasse, F.; Maier, M. E. *Chem.—Eur. J.* **2011**, *17*, 13349−13357.
(42) Tannert, R.; Milroy, L.-G.; Ellinger, B.; Hu, T.-S.; Arndt, H.-D.; Waldmann, H. *J. Am. Chem. Soc.* **2010**, *132*, 3063.
(43) Waldmann, H.; Hu, T.-S.; Renner, S.; Menninger, S.; Tannert, R.; Oda, T.; Arndt, H.-D. *Angew. Chem., Int. Ed.* **2008**, *47*, 6473.
(44) Gala, F.; D'Auria, M. V.; De Marino, S.; Zollo, F.; Smith, C. D.; Copper, J. E.; Zampella, A. *Tetrahedron* **2007**, *63*, 5212.
(45) Gala, F.; D'Auria, M. V.; De Marino, S.; Sepe, V.; Zollo, F.; Smith, C. D.; Copper, J. E.; Zampella, A. *Tetrahedron* **2008**, *64*, 7127.
(46) Gala, F.; D'Auria, M. V.; De Marino, S.; Sepe, V.; Zollo, F.; Smith, C. D.; Keller, S. N.; Zampella, A. *Tetrahedron* **2009**, *65*, 51.
(47) Oda, T.; Namba, K.; Maéda, Y. *Biophys. J.* **2005**, *88*, 2727.
(48) Steinmetz, M. O.; Stoffler, D.; Müller, S. A.; Jahn, W.; Wolpensinger, B.; Goldie, K. N.; Engel, A.; Faulstich, H.; Aebi, U. *J. Mol. Biol.* **1998**, *276*, 1.
(49) Klebe, R. J.; Ruddle, F. H. *J. Cell Biol.* **1969**, *43*, 69A.
(50) Axelrod, D. *J. Cell Biol.* **1981**, *89*, 141.
(51) Hotulainen, P.; Lappalainen, P. *J. Cell Biol.* **2006**, *173*, 383.
(52) Bubb, M. R.; Spector, I.; Beyer, B. B.; Fosen, K. M. *J. Biol. Chem.* **2000**, *275*, 5163.
(53) van Goor, D.; Hylland, C.; Schaefer, A. W.; Forscher, P. *PLoS One* **2012**, *7*, e30959.
(54) de la Cruz, E. M.; Pollard, T. D. *Biochemistry* **1994**, *33*, 14387.
(55) Schaefer, A. W.; Kabir, N.; Forscher, P. *J. Cell. Biol.* **2002**, *158*, 139.